PHILOSOPHICAL MAGAZINE B, 2000, VOL. 80, NO. 5, 897–905

Current-biased inductive cubic networks of Josephson junctions

R. DE LUCA†, T. DI MATTEO

Istituto Nazionale per la Fisica della Materia and Dipartimento di Fisica
Universitá degli Studi di Salerno, I-84081 Baronissi (Salerno), Italy

A. TUOHIMAA and J. PAASI

Laboratory of Electromagnetics, Tampere University of Technology,
FIN-33101 Tampere, Finland

ABSTRACT

The electrodynamic response of a current-biased inductive network of small Josephson junctions located at the edges of a cube of side a is studied. The dynamical equations for the gauge-invariant phase differences across the junctions are derived in the presence of a constant magnetic field $\mathbf{H}$ applied along an arbitrary direction in space. When $\mathbf{H}$ is applied in a direction parallel to one of the sides, it is found that the time evolution of the voltages across the branches of the network reproduces the well known features present in superconducting quantum interference devices.

§1. INTRODUCTION

The electrodynamics of Josephson junction networks has been studied since the 1980s (Nahajima and Sawada 1981, Lobb *et al.* 1983, Ebner and Stroud 1985). After the discovery of high-T_c superconductors (Bednorz and Muller 1996), these networks were adopted as equivalent circuits for the study of the physical properties of this new class of materials (Clem 1988, Tinkham and Lobb 1989). However, the attention of researchers was mainly devoted to one-dimensional or two-dimensional Josephson junction arrays (Phillips *et al.* 1993, Wolf and Majhofer 1993, Auletta *et al.* 1994, Chen *et al.* 1994, Paasi *et al.* 1996). Only more recently, has the electrodynamic response of three-dimensional (3D) Josephson junction networks been investigated (Yukon and Lin 1995, De Luca *et al.* 1998).

Among the electronic devices modelled through simple Josephson junction networks we can mention the superconducting quantum interference device (SQUID). SQUIDs are versatile magnetic field sensors, finding applications in biomagnetic measurements, such as magnetoencephalography (Hämäläinen *et al.* 1993) and magnetocardiography (Rijpma *et al.* 1997), as well as in geophysical monitoring (Dantsker *et al.* 1994) and in non-destructive maintenance testing of aircrafts (Krause *et al.* 1997). These devices, owing to their planar geometry, can detect only one field component. On the other hand, a current-biased 3D Josephson junc-

†E-mail: deluca@physics.unisa.it

Philosophical Magazine B ISSN 0141–8637 print/ISSN 1463–6417 online © 2000 Taylor & Francis Ltd
http://www.tandf.co.uk/journals/tf/01418637.html

tion network could be adopted as a model of a 3D device able to detect the complete vectorial nature of an externally applied magnetic field $\mathbf{H}$.

In the present paper we therefore study the electrodynamic response of a current-biased inductive cubic network of small Josephson junctions. In § 2 we write the complete set of equations governing the dynamics of the gauge-invariant phase differences across the junctions. In § 3 we solve the resulting nonlinear ordinary differential equations by a standard numerical procedure and, by relating the phase variables to observable electrodynamic quantities, we show that the system's behaviour is similar to that of a SQUID in the case when $\mathbf{H}$ is aligned with the direction of one cubic side. Finally, voltage–current $(V\text{-}I)$ curves are derived for different field orientations. Conclusions are drawn in the last section.

§ 2. Equations

A current-biased cubic network of inductively coupled Josephson junctions is shown in figure 1. A Josephson junction is placed at the midpoint of each branch of the network. The superconducting state of each junction is defined through the gauge-invariant phase difference $\varphi_\xi(\mathbf{r})$, where $\mathbf{r} = (x,y,z)$ denotes the position of the junction and ξ is the direction along which the junction lies. In order to take account of the magnetic energies of the branch currents $i_\xi(\mathbf{r})$, an inductor of inductance L is placed on each branch of the network. The dynamical equations for the $\varphi_\xi(\mathbf{r})$ values can be derived with the aid of the resistively shunted junction (RSJ) model (Barone and Paternó 1982). By neglecting capacitive effects in the junction and by considering a homogeneous network, we can define a nonlinear Josephson operator

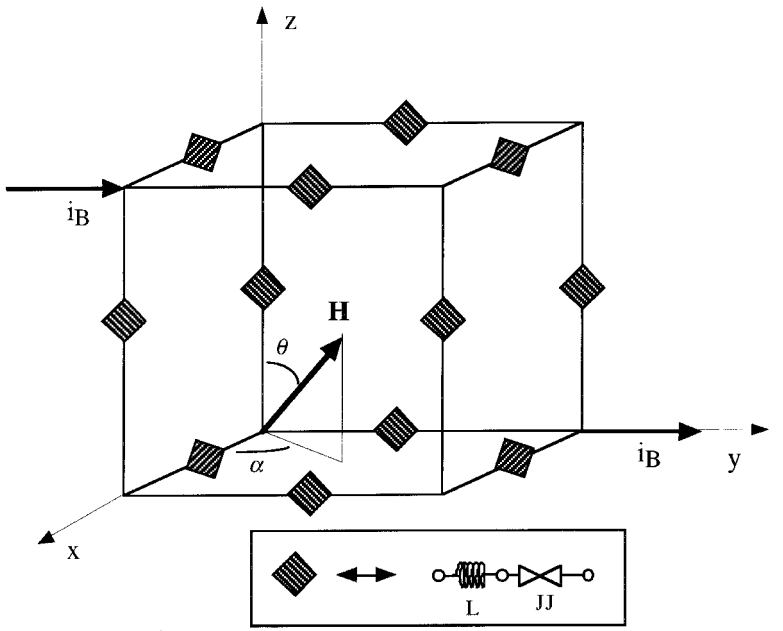

Figure 1. Current-biased 3D Josephson junction network. The current is injected at node $(a,0,a)$ and is drawn at node $(0,a,0)$. Each box in the network contains a resistively shunted junction and an inductor, as is shown in the lower part of the figure.

$$O_J(\cdot) = \frac{\Phi_0}{2\pi R}\frac{d}{dt}(\cdot) + I_J \sin(\cdot), \tag{1}$$

where Φ_0 is the elementary flux quantum and where R and I_J are the resistive parameter and the maximum Josephson current respectively of each junction in the network. In this way, the 12 dynamical equations for the phase variables can be written as follows

$$O_J[\Phi_\xi(\mathbf{r})] = i_\xi(\mathbf{r}). \tag{2}$$

The currents appearing on the right-hand side of equation (2) can now be expressed in terms of the phase variables according to the following procedure.

First, write the fluxoid quantization relations. Let us then consider a cubic structure as the result of a given number of translations of a triad of mutually orthogonal adjacent squares of side a with a common point in the origin. The generic magnetic flux through the cubic face parallel to the μ-ν plane (μ-$\nu = y$-z, z-x, x-y) of the triad having a common point in $\mathbf{r}$ can be denoted by $\Phi_{\mu\nu}(\mathbf{r})$. In this way, we can write

$$\frac{2\pi}{\Phi_0}\Phi_{\mu\nu}(\mathbf{r}) = 2\pi n_{\mu\nu}(\mathbf{r}) + \Theta_{\mu\nu}, \tag{3}$$

where $n_{\mu\nu}(\mathbf{r})$ is an integer and

$$\Theta_{\mu\nu} = \varphi_\mu(\mathbf{r} + a\hat{\nu}) - \varphi_\mu(\mathbf{r}) - \varphi_\nu(\mathbf{r} + a\hat{\mu}) + \varphi_\nu(\mathbf{r}), \tag{4}$$

$\hat{\eta}$ being the unit vector in the generic η direction. Note that, because of Maxwell equation $\nabla\cdot\mathbf{B} = 0$, only five fluxoid quantization relations are independent.

Next, express the fluxes $\Phi_{\mu\nu}(\mathbf{r})$ in terms of the branch currents and of the externally applied flux $\mu_0\mathbf{H}\cdot\mathbf{S}_{\mu\nu}(\mathbf{r})$, where $\mathbf{S}_{\mu\nu}(\mathbf{r})$ is the area vector oriented in the positive ξ direction ($\xi \neq \mu, \nu$), so that $\mathbf{S}_{\mu\nu}(\mathbf{r} + \hat{\xi}) = \mathbf{S}_{\mu\nu}(\mathbf{r}) = a^2\hat{\xi}$. Adding now the effects of the branch currents and of the external field $\mathbf{H}$, we have

$$\begin{aligned}\Phi_{\mu\nu}(\mathbf{r}) &= LI_{\mu\nu}(\mathbf{r}) + MI_{\mu\nu}(\mathbf{r} + a\hat{\xi}) + \mu_0\mathbf{H}\cdot\mathbf{S}_{\mu\nu}(\mathbf{r}),\\ \Phi_{\mu\nu}(\mathbf{r} + a\hat{\xi}) &= LI_{\mu\nu}(\mathbf{r} + a\hat{\xi}) + MI_{\mu\nu}(\mathbf{r}) + \mu_0\mathbf{H}\cdot\mathbf{S}_{\mu\nu}(\mathbf{r}),\end{aligned} \tag{5}$$

where M is proportional to the mutual inductance coefficient between two parallel loops and

$$I_{\mu\nu}(\mathbf{r}) = i_\mu(\mathbf{r}) - i_\mu(\mathbf{r} + a\hat{\nu}) + i_\nu(\mathbf{r} + a\hat{\mu}) - i_\nu(\mathbf{r}). \tag{6}$$

In order to carry out calculations explicitly, we rewrite equations (2)–(6) in matrix form. By defining

$$\mathbf{I}_S = \begin{pmatrix} I_{yz}(0)\\ I_{yz}(a\hat{x})\\ I_{zx}(0)\\ I_{zx}(a\hat{y})\\ I_{xy}(0)\end{pmatrix}, \qquad \boldsymbol{\Phi} = \begin{pmatrix} \Phi_{yz}(0)\\ \Phi_{yz}(a\hat{x})\\ \Phi_{zx}(0)\\ \Phi_{zx}(a\hat{y})\\ \Phi_{xy}(0)\end{pmatrix}, \qquad \boldsymbol{\Phi}_{ex} = \mu_0 a^2\begin{pmatrix} \mathbf{H}\cdot\hat{\mathbf{x}}\\ \mathbf{H}\cdot\hat{\mathbf{x}}\\ \mathbf{H}\cdot\hat{\mathbf{y}}\\ \mathbf{H}\cdot\hat{\mathbf{y}}\\ \mathbf{H}\cdot\hat{\mathbf{z}}\end{pmatrix}, \tag{7}$$

we can rewrite equations (5) as follows:

$$\boldsymbol{\Phi} = \mathbf{G}\mathbf{I}_S + \boldsymbol{\Phi}_{ex}, \tag{8}$$

where $\mathbf{G}$ is the following 5×5 matrix:

$$\mathbf{G} = \begin{pmatrix} L & M & 0 & 0 & 0 \\ M & L & 0 & 0 & 0 \\ 0 & 0 & L & M & 0 \\ 0 & 0 & M & L & 0 \\ M & -M & M & -M & (L+M) \end{pmatrix}. \tag{9}$$

Note that $\mathbf{G}$ is non-singular, so that

$$\mathbf{I}_S = \mathbf{G}^{-1}(\boldsymbol{\Phi} - \boldsymbol{\Phi}_{ex}). \tag{10}$$

If no flux is trapped in the system at $\mathsf{H} = 0$, we can set $n_{\mu\nu} = 0$ in equation (3). In this way we can write

$$\boldsymbol{\Phi} = \frac{\Phi_0}{2\pi}\mathbf{F}\boldsymbol{\varphi}, \tag{11}$$

where $\mathbf{F}$ is a 5×12 matrix and $\boldsymbol{\varphi}$ is a column vector whose components are the 12 phase differences $\varphi_\xi(\mathsf{r})$. The elements of $\mathbf{F}$ are either zeros or ± 1. By equation (6) we can now write

$$\mathbf{I}_S = -\mathbf{F}\mathsf{i}, \tag{12}$$

where i is a column vector, whose components are the 12 branch currents. Because of charge conservation at the nodes, we can express the 12 components of i in terms of five independent branch currents, forming a column vector i_I, and in terms of a 12 component vector I_B, which can be made explicit once the nodes at which the current is injected and drawn are defined. Therefore, one can write

$$\mathsf{i} = \mathbf{T}\mathsf{i}_\mathrm{I} - \mathsf{I}_\mathrm{B}, \tag{13}$$

where $\mathbf{T}$ is a 12×5 matrix with elements $T_{ij} = 0, \pm 1$ and where the transpose of I_B is

$$(\mathsf{I}_\mathrm{B})^\mathrm{T} = (0 \;\; i_\mathrm{B} \;\; 0 \;\; 0 \;\; 0 \;\; 0 \;\; 0 \;\; -i_\mathrm{B} \;\; 0 \;\; 0 \;\; 0 \;\; i_\mathrm{B}) \tag{14}$$

for the bias current configuration chosen in figure l. By combining equations (10)–(14) we can write equation (2) symbolically as follows:

$$O_\mathrm{J}(\boldsymbol{\varphi}) + \frac{\Phi_0}{2\pi}\mathbf{A}\boldsymbol{\varphi} = \mathbf{B}\boldsymbol{\Phi}_{ex} + (\mathbf{C} - \mathbf{I})\mathsf{I}_\mathrm{B}, \tag{15}$$

where

$$\begin{aligned} \mathbf{A} &= \mathbf{T}(\mathbf{FT})^{-1}\mathbf{G}^{-1}\mathbf{F}, \\ \mathbf{B} &= \mathbf{T}(\mathbf{FT})^{-1}\mathbf{G}^{-1}, \\ \mathbf{C} &= \mathbf{T}(\mathbf{FT})^{-1}\mathbf{F}, \end{aligned} \tag{16}$$

and where $\mathbf{I}$ is the 12×12 identity matrix.

The set of nonlinear ordinary differential equations given in equation (15) defines the dynamics of the 12 Josephson junctions in the current-biased network of figure 1.

§ 3. Observable quantities

Having derived the dynamical equations for the phase variables in the previous section, we may now turn to the problem of calculating physically observable quantities. One observable quantity is the time average of the voltage $V_\xi(\mathsf{r}, t)$, for which indexing is the same as for branch currents, except for the explicit time dependence,

which will appear in all quantities in this section, whenever it applies. The voltage $V_\xi(\mathbf{r},t)$ across a branch lying in the ξ direction can be defined as follows:

$$V_\xi(\mathbf{r},t) = \frac{\Phi_0}{2\pi}\frac{\mathrm{d}\varphi_\xi}{\mathrm{d}t}(\mathbf{r},t) + L\,\frac{\mathrm{d}i_\xi}{\mathrm{d}t}(\mathbf{r},t). \tag{17}$$

Numerically, time averaging can be computed, starting from the usual definition

$$\langle V_\xi(\mathbf{r})\rangle = \frac{1}{T}\int_0^{\mathrm{T}} V_\xi(\mathbf{r},t)\,\mathrm{d}t, \tag{18}$$

by summing voltages over a large time interval T and then by dividing by the number of terms in the summation. However, if $V_\xi(\mathbf{r},t)$ is a periodic function with period T_ξ, we can replace T with T_ξ in equation (18). In this last case,

$$\langle V_\xi(\mathbf{r})\rangle = \frac{\Phi_0}{2\pi T_\xi}\left[\varphi_\xi(\mathbf{r},T_\xi) - \varphi_\xi(\mathbf{r},0)\right] + \frac{L}{T_\xi}\left[i_\xi(\mathbf{r},T_\xi) - i_\xi(\mathbf{r},0)\right]. \tag{19}$$

It can be shown that, in the case when $\mathbf{H} = H\hat{\mathbf{z}}$ and for bias currents greater than the maximum current $I_{\mathrm{B}}^{\max} = 3I_{\mathrm{J}}$, the voltages $V_\xi(\mathbf{r},t)$ are periodic. In figure 2 we report the normalized voltages $v_x(0,t) = V_x(0,t)/RI_{\mathrm{J}}$ and $v_x(a\hat{\mathbf{y}},t) = V_x(a\hat{y},t)/RI_{\mathrm{J}}$, for which a clear periodicity can be detected. The same can be shown for the currents $i_\xi(\mathbf{r},t)$. In this way, equation (19) becomes

$$\langle V_\xi(\mathbf{r})\rangle = \frac{\Phi_0}{2\pi T_\xi}\,\Delta\varphi_\xi, \tag{20}$$

where $\Delta\varphi_\xi = \varphi_\xi(\mathbf{r},T_\xi) - \varphi_\xi(\mathbf{r},0)$. In figure 3 we show how the normalized voltage $v_x(0,t)$ varies for different applied field amplitudes, namely for $\Psi_{\mathrm{ex}} = 2.0$ and for $\Psi_{\mathrm{ex}} = 2.5$, where $\Psi_{\mathrm{ex}} = \mu_0 H a^2/\Phi_0$.

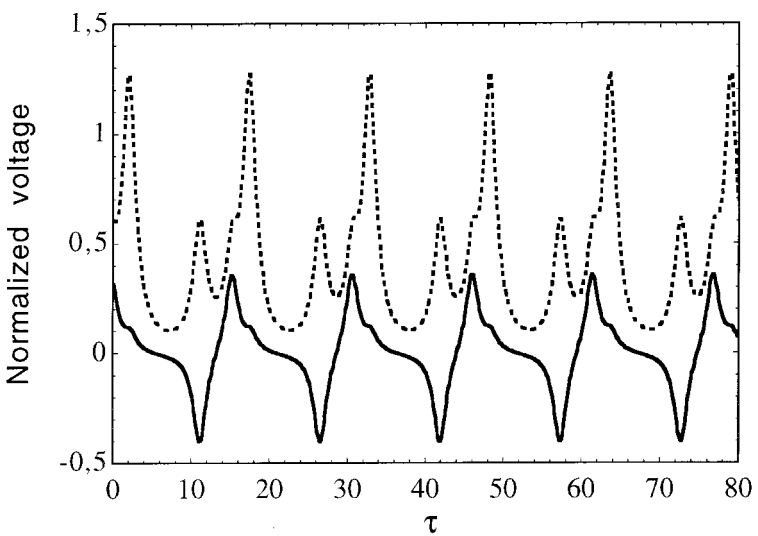

Figure 2. Normalized voltages $v_x(\mathbf{r},t) = V_x(\mathbf{r},t)/RI_{\mathrm{J}}$ for $\mathbf{H} = H\hat{\mathbf{z}}$, $\beta = LI_{\mathrm{J}}/\Phi_0 = 1.4$, $i_{\mathrm{B}} = 3.2I_{\mathrm{J}}$ and $\Psi_{\mathrm{ex}} = 2.5$, where the normalized time is $\tau = 2\pi RI_{\mathrm{J}}t/\Phi_0$: (——), $v_x(\mathbf{r} = \mathbf{0},t)$; (- - - - -), $v_x(a\hat{\mathbf{y}},t)$.

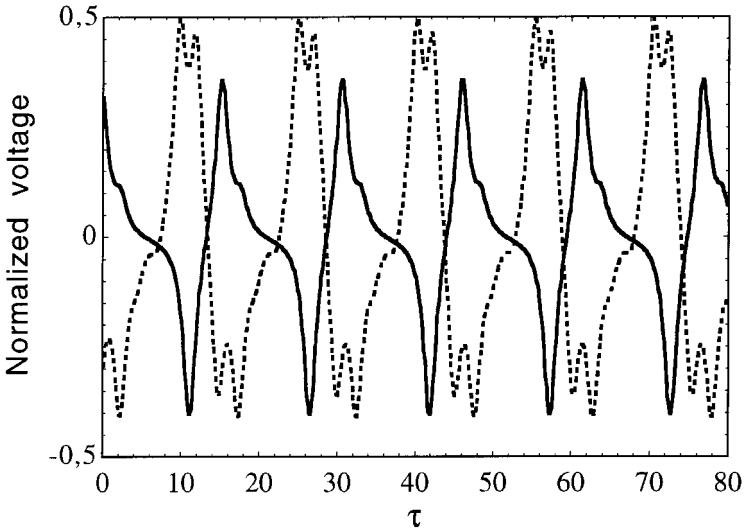

Figure 3. Normalized voltages $v_x(\mathbf{r}=\mathbf{0},t)=V_x(\mathbf{r}=\mathbf{0},t)/RI_J$ for $\mathbf{H}=H\hat{\mathbf{z}}$, $\beta=LI_J/\Phi_0=1.4$, $i_B=3.2I_J$ and for $\Psi_{ex}=2.5$ (——) and $\Psi_{ex}=2.0$ (- - - - -), where the normalized time is $\tau=2\pi RI_Jt/\Phi_0$.

In order to stress the analogy with SQUIDs, we show the V-I characteristics of the system for field directions along one of the coordinate axes. The V-I curves are calculated numerically by means of a standard fourth-order Runge–Kutta algorithm. In figure 4 we show V-I characteristics of all branches for $\Psi_{ex}=0$ and for $\beta=LI_J/\Phi_0=1.4$. Here the presence of two positive branches together with their symmetric negative counterparts should be noted. These branches correspond to the only possible values of the currents in the network, namely $\pm i_B/6$ and $\pm i_B/3$. In this case, the phase difference $\varphi_\xi(\mathbf{r},t)$ goes through a 2π phase shift in the time interval $[t_0,t_0+T_\xi]$ when the junction is in the running state. It is then possible to derive an analytic expression for the V-I curves, by setting

$$O_J(\varphi_\xi(\mathbf{r},t))=K, \tag{21}$$

where $K=\pm i_B/6, \pm i_B/3$, and by integrating equation (21) by separation of variables (Barone and Paternó 1982) to obtain

$$\langle v_\xi\rangle=\pm(k^2-1)^{1/2}, \tag{22}$$

where $\langle v_\xi\rangle=\langle V_\xi\rangle/RI_J$ is the normalized average voltage and $k=(K/I_J)>1$.

In figure 5 we show a comparison between two V-I curves: one obtained for $\Psi_{ex}=0$ and the second obtained for $\Psi_{ex}=0.5$. From these graphs it should be noted that the maximum bias current I_B^{max} which can be injected in the network before causing phase slip of the junctions depends on the applied flux number Ψ_{ex}. A similar behaviour of I_B^{max} can be seen in the V-I curves shown in figure 6 for the magnetic field direction given by the azimuth angle $\alpha=0$ and by the zenith angle $\theta=\pi/6$.

The above preliminary study of the observable quantities in current-biased inductive cubic networks of Josephson junctions allowed us to derive V-I curves

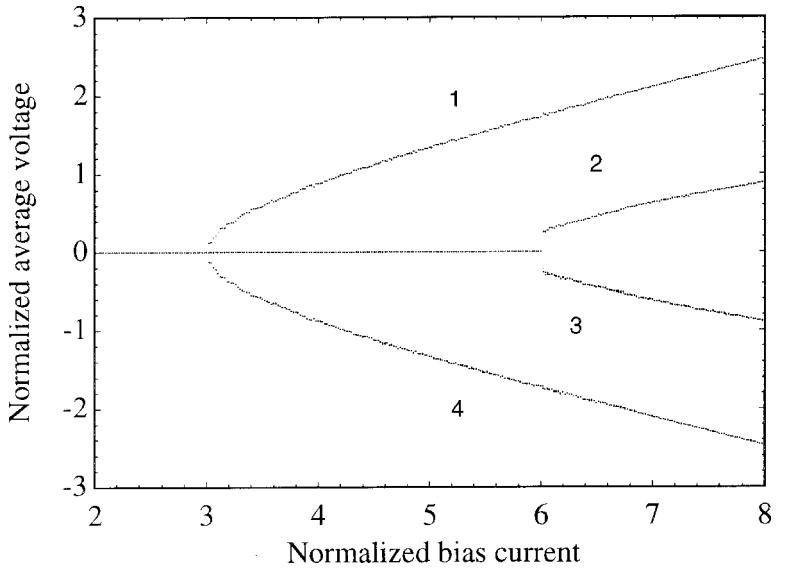

Figure 4. V-I characteristics of the cubic network of Josephson junctions for $\mathbf{H} = \mathbf{0}$, and $\beta = LI_J/\Phi_0 = 1.4$. Branch 1 corresponds to the normalized average voltages $\langle v_y(\mathbf{r} = \mathbf{0})\rangle$ and $\langle v_y(\mathbf{r} = a\hat{\mathbf{x}} + a\hat{\mathbf{z}})\rangle$; branch 2 corresponds to the normalized average voltages $\langle v_y(\mathbf{r} = a\hat{\mathbf{x}})\rangle$ and $\langle v_y(\mathbf{r} = a\hat{\mathbf{z}})\rangle$; branch 3 corresponds to the normalized average voltages $\langle v_x(\mathbf{r} = \mathbf{0})\rangle$, $\langle v_z(\mathbf{r} = \mathbf{0})\rangle$, $\langle v_x(\mathbf{r} = a\hat{y} + a\hat{\mathbf{z}})\rangle$ and $\langle v_z(\mathbf{r} = a\hat{x} + a\hat{\mathbf{y}})\rangle$; finally branch 4 corresponds to the normalized average voltages $\langle v_x(\mathbf{r} = a\hat{\mathbf{z}})\rangle$, $\langle v_z(\mathbf{r} = a\hat{\mathbf{x}})\rangle$, $\langle v_x(\mathbf{r} = a\hat{\mathbf{y}})\rangle$ and $\langle v_z(\mathbf{r} = a\hat{\mathbf{y}})\rangle$.

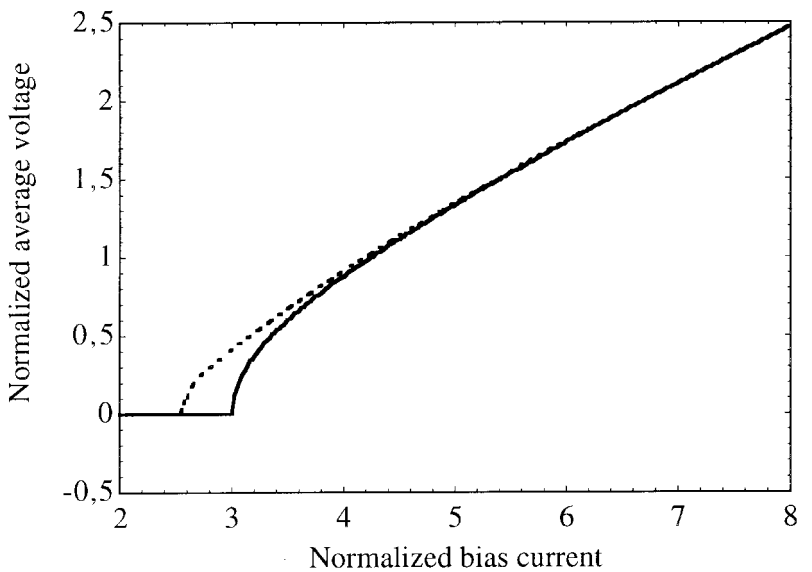

Figure 5. Comparison between V-I curves of the cubic network of Josephson junctions obtained for $\beta = LI_J/\Phi_0 = 0.4$ and for $\Psi_{ex} = 0$ (——) and $\Psi_{ex} = 0.5$ (- - - - -). The voltage shown is $\langle v_y(\mathbf{r} = \mathbf{0})\rangle$ and the field $\mathbf{H}$ is applied in the z direction.

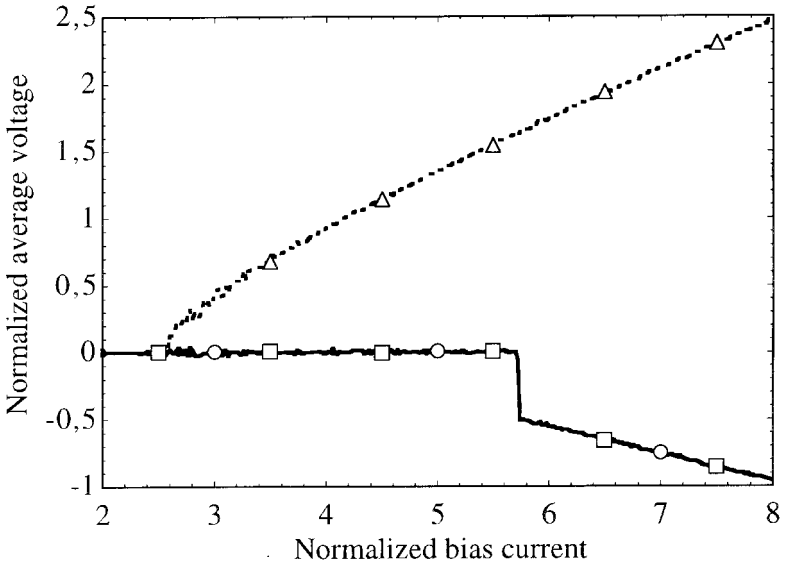

Figure 6. V-I curves of the cubic network of Josephson junctions obtained at the field orientation $\alpha = 0$ and $\theta = \pi/6$ and for $\beta = LI_J/\Phi_0 = 0.4$ and $\Psi_{ex} = 0.8$. The normalized average voltages shown are $\langle v_x(\mathbf{r} = \mathbf{0})\rangle$ (○), $\langle v_y(\mathbf{r} = \mathbf{0})\rangle$ (△) and $\langle v_z(\mathbf{r} = \mathbf{0})\rangle$ (□).

for the bias current configuration shown in figure 1. Starting from the periodicity of the voltages across each branch of the network for bias currents greater than I_B^{max}, we were able to derive an analytic expression for V-I curves in the absence of an externally applied field. On the other hand, for magnetic fields directed along one of the coordinate axis, the cubic system is seen to show a behaviour similar to dc SQUIDs, even though the flux dynamics are more complex in the former. V-I curves obtained for fields lying in the x-z plane and oriented at an angle θ with respect to the z axis show that the current I_B^{max} depends on θ. This last aspect is due to different shielding current distributions arising in the 3D system as the orientation of $\mathbf{H}$ is changed. Because of these features, the network could be considered a model system of a vectorial magnetic field sensor. However, owing to the intrinsic complexity of the problem, further studies are required.

§4. Conclusions

We studied the electrodynamic response of a current-biased inductive network of small Josephson junctions in the presence of an external magnetic field $\mathbf{H}$. The system's equations were derived in a general way, so that they can be applied to the same network with a different current bias configuration. We numerically evaluated the voltages across each branch of the network and V-I curves for the bias current configuration shown in figure 1. It should be noted that, for zero applied field, the V-I curves can be derived analytically. For non-zero field amplitudes H and for different field orientations $\hat{\mathbf{H}}$, on the other hand, these curves are seen to depend on both H and $\hat{\mathbf{H}}$. Because of the complexity of the problem, however, further investigation is needed in order to confirm the potentialities to adopt this network as a model of a vectorial magnetic field sensor.

REFERENCES

AULETTA, C., RAICONI, G., DE LUCA, R., and PACE, S., 1994, *Phys. Rev.* B, **49**, 12 311.
BARONE, A., and PATERNÓ, G., 1982, *Physics and Applications of the Josephson Effect* (New York: Wiley).
BEDNORZ, J. G., and MULLER, K. A., 1986, *Z. Phys.* B, **64**, 189.
CHEN, D. X., SANCHEZ, A., and HERNANDO, A., 1994, *Phys. Rev.* B, **50**, 13 735.
CLEM, J.R., 1988, *Physica* C, **153–155**, 50.
DANTSKER, E., KOELLE, D., MIKLICH, A. H., NEMETH, D. T., LUDWIG, F., and CLARKE, J., 1994, *Rev. scient. Instrum.,* **65**, 3809.
DE LUCA, R., DI MATTEO, T., TUOHIMAA, A., and PAASI, J., 1998, *Phys. Rev.* B, **57**, 1173.
EBNER, C., and STROUD, D., 1985, *Phys. Rev.* B, **31**, 165.
HÄMALAINEN, M., HARI, R., ILMONIEMI, R. J., KNUUTILA, J., and LOUNASMA, O. V., 1993, *Rev. mod. Phys.,* **65**, 413.
KRAUSE, H.-J., ZANG, Y., HOHMANN, R., GRUNEKLEE, M., FALEY, M. I., LOMPARSKI, D., MAUS, M., BOUSACK, H., and BRAGINSKI, A. I., 1997, *Inst. Phys. Conf. Ser.,* **158**, 775.
LOBB, C. J., ABRAHAMS, D. W., and TINKHAM, M., 1983, *Phys. Rev.* B, **27**, 150.
NAKAJIMA, K., and SAWADA, Y., 1981, *J. appl. Phys.,* **52**, 5732.
PAASI, J., TUOHIMAA, A., and ERIKSSON, J.-T., 1996, *Physica* C, **259**, 10.
PHILLIPS, J. R., VAN DER ZANT, H. S. J., WHITE, J., and ORLANDO, T. P., 1993, *Phys. Rev.* B, **47**, 5219.
RIJPMA, A. P., SEPPENWOOLDE, Y., TER BRAKE, H. J. M., PETERS, M. J., and ROGALLA, H., 1997, *Inst. Phys. Conf. Ser.,* **158**, 771.
TINKHAM, M., and LOBB, C. J., 1989, *Solid St. Phys.,* **42**, 91.
WOLF, T., and MAJHOFER, A., 1993, *Phys. Rev.* B, **47**, 7481.
YUKON, S. P., LIN, N., and CHU H., 1995, *IEEE Trans. appl. Supercond.,* **5**, 2959.